

OPEN ACCESS

Structure of OH⁻ defects in LiNbO₃

To cite this article: K Lengyel *et al* 2010 *IOP Conf. Ser.: Mater. Sci. Eng.* **15** 012015

View the [article online](#) for updates and enhancements.

You may also like

- [A Highly Hydroxide Conductive, Chemically Stable Anion Exchange Membrane. Poly\(2,6 dimethyl 1,4 phenylene oxide\)-b-Poly\(vinyl benzyl trimethyl ammonium\), for Electrochemical Applications](#)
Tara P. Pandey, Himanshu N. Sarode, Yating Yang et al.
- [Gamma-radiation effects in pure-silica-core photonic crystal fiber](#)
Wei Cai, , Ningfang Song et al.
- [The Mechanism of the Zinc\(II\)/Zinc Amalgam Electrode Reaction in Alkaline Media As Studied by Chronocoulometric and Voltammetric Techniques](#)
DeWitt A. Payne and Allen J. Bard



ECS
The
Electrochemical
Society
Advancing solid state &
electrochemical science & technology

DISCOVER
how sustainability
intersects with
electrochemistry & solid
state science research

Structure of OH⁻ defects in LiNbO₃

K Lengyel¹, V Timón², A Hernández-Laguna², V Szalay¹ and
L Kovács¹

¹ Research Institute for Solid State Physics and Optics, Hungarian Academy of Sciences,
P. O. Box 49, H-1525 Budapest, Hungary

² Instituto Andaluz de Ciencias de la Tierra (IACT-UGR), Granada, Spain

E-mail: klengyel@szfki.hu

Abstract. The geometry of the most stable configuration of OH⁻ defects in nearly stoichiometric, hydrogen-contaminated, LiNbO₃ has been determined from first principles theoretical calculations. In the most stable configuration the proton is located near a bisector of an oxygen triangle and is tilted by 4.3 degrees out of the oxygen plane towards a lithium vacancy. The equilibrium length of the OH⁻ bond has been found to be 0.988 Å.

1. Introduction

Investigations into the structure and dynamical properties of LiNbO₃ single crystals are motivated by the wealth of potential practical applications resulting from the remarkable physical properties of LiNbO₃. Dopants and impurities can significantly influence the physical properties of crystals, thereby enhancing or hindering their practical utility. In particular, hydrogen, a contaminant, built into LiNbO₃ during the growth process as an OH⁻ ion, is believed to be responsible for thermal fixing of optical holograms. Partly, it is for this reason, that great effort has been expended on studying the OH⁻ defect in LiNbO₃ crystals, and a large body of experimental data has been accumulated [1, 2]. The experimental data have been analyzed by employing simplified, phenomenological models [1, 2, 3, 4], and there have been only few attempts [5] to analyse and supplement them by first principles theoretical calculations.

Vibrational spectroscopy has given dynamical information such as transition frequencies, intensities, and the shape of the potential energy surface (PES) related to vibrations of protons caged in the crystal lattice [2, 4]. Some dynamical and kinetical information, namely activation barrier height and rate constants, have been deduced from analysing results of temperature dependent electric conductivity [6] and infrared (IR) spectra [7] as well as holographic scattering [8]. ¹H nuclear magnetic resonance (NMR) measurements have been employed to find out the location of protons within the crystal lattice [9, 10, 11].

We have undertaken a combined experimental and theoretical investigation of proton dynamics in LiNbO₃ single crystals. A prerequisite to dynamical studies of nuclear motions, except Carr-Parrinello type calculations, is to obtain reliable structural data and potential energy surfaces.

In this communication we report our results on the geometry and potential energy surface of OH⁻ defects in nearly stoichiometric, hydrogen-contaminated, LiNbO₃ obtained from first principles calculations.

The paper is organized as follows. Section 2. describes the type of calculations carried out and discusses the results. Technical details of the calculations are outlined in an Appendix. Section 3. summarizes the results.

2. The structure of OH^- defects in LiNbO_3

Proton dynamics is assumed to take place under the influence of a PES derived via the Born-Oppenheimer approximation. That is the PES is defined as the total energy given as a function of the coordinates of the nuclei. More precisely, it is the electronic energy in the ground electronic state depending parametrically on the coordinates of the nuclei plus the nucleon-nucleon repulsion energy.

To model the crystal a supercell composed of $2 \times 2 \times 2$ hexagonal unit cells (240 atoms) along with periodic boundary conditions has been employed. The structure of the supercell has been fully optimized by taking as the initial geometry that of a supercell built from the unit cell of stoichiometric LiNbO_3 . The structural data for the unit cell of stoichiometric LiNbO_3 are taken from Ref. [12]. Only very small deviations have been found between the fully relaxed and initial supercell geometries.

Our goal is to find the OH^- defect cluster of the most stable configuration. Since simply introducing a hydrogen atom into the supercell gives configurations of much higher energy than that of configurations one obtains by simultaneous introduction of a hydrogen atom into and removing of a lithium atom from the innermost part of the supercell, it suffices to consider only clusters of the latter type.

Thus placing the hydrogen atom in various positions within the supercell and calculating the total energy one can map the PES of proton dynamics. The location of the deepest minimum of this surface defines the equilibrium geometry of the OH^- defect.

Introduction of defects can distort the structure of the supercell. Therefore, we have carried out geometry optimization of the supercell with an OH^- defect by letting all nuclei move within the supercell. But the proton all other nuclei (ions) have remained essentially in their initial positions. Then, by placing the proton in different locations within this relaxed-geometry configuration the PES has been sampled.

Although geometry relaxation should have been carried out at each configuration, it is expected that in spite of this approximation the resulting PES will be accurate enough to account for most of the spectroscopic experimental data.

We have mapped the PES on a grid of 2251 points depicted in Fig. 1.

Then by employing these sample points an analytical approximating PES has been constructed. 1D cuts and 2D levelsets of the 3D analytical approximating PES are shown in Figs. 2 and 3, respectively.

One can clearly recognize that one of the proton vibrational modes, the one which can be associated with the OH^- stretch, takes place, at least in the first approximation, in a Morse-like potential curve. This justifies the use of Morse potential when analysing the OH^- stretch related IR transitions of LiNbO_3 . Further results on dynamical issues will be discussed in another publication.

Besides dynamics, the PES gives information on the location of proton within the crystal lattice. The coordinates of the global minimum of the PES as given in the Cartesian system of axes X, Y, Z shown in Fig. 1 are $X_{eq} = 2.1263 \text{ \AA}$, $Y_{eq} = 5.28064 \text{ \AA}$, and $Z_{eq} = 10.15354 \text{ \AA}$. The distance of the hydrogen from the nearest oxygen, the equilibrium OH^- bond length, is $r_{eq} = 0.988 \text{ \AA}$, which may be worth comparing with the bond length one would obtain by employing the method of Ref. [13].

Our results show that in the most stable configuration the proton is neither on, nor in the vicinity of a line connecting nearest neighbour oxygens (denoted by O-O), but it is located near

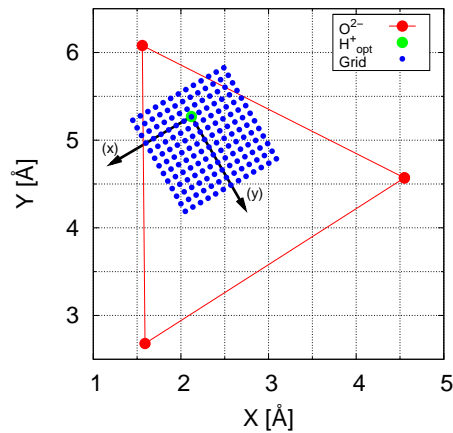


Figure 1. Grid points employed to sample the PES of proton dynamics. 2251 grid points, $P_i = (X_i, Y_i, Z_i)$, $i = 1, 2, \dots, 2251$, have been chosen. In addition to the initial Cartesian system of axes, (X, Y, Z) we also employed the Cartesian system (x, y, z) depicted.

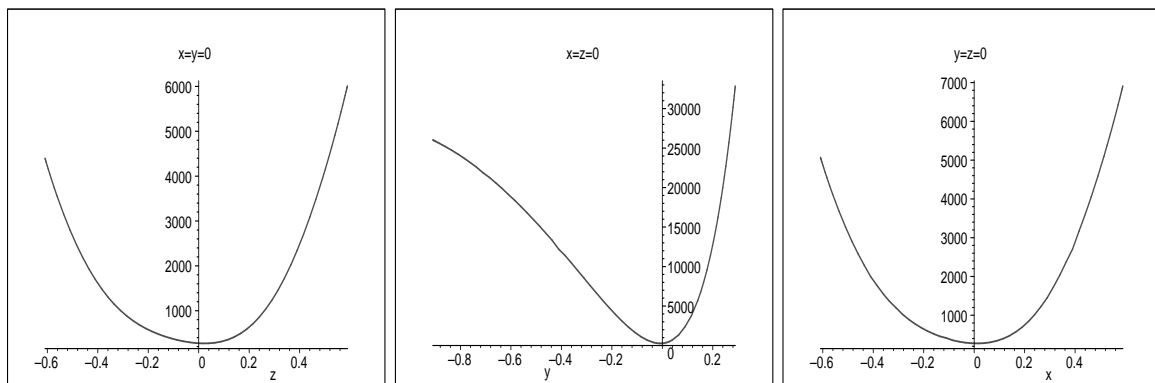


Figure 2. 1D cuts of the 3D analytical approximating PES of proton dynamics. Energy (vertical axis) is measured in units of wavenumbers and it is given as a function of proton coordinates z , y , and x , respectively. The coordinates of the proton are in units of \AA , and given in the (x, y, z) Cartesian coordinate system shown in Fig. 1

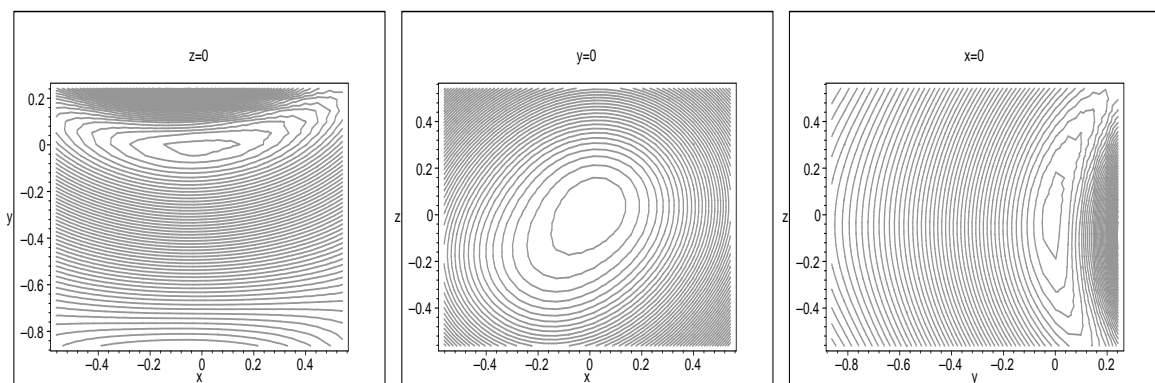


Figure 3. 2D cuts and levelsets of the 3D analytical approximating PES of proton dynamics.

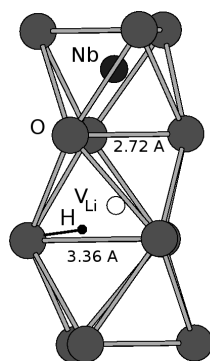


Figure 4. The most stable configuration, where the proton is located near a bisector of an oxygen triangle (3.36 Å) and is tilted by 4.3 degrees out of the oxygen plane towards the lithium vacancy.

a bisector of an oxygen triangle, and it is tilted by 4.3 degrees out of the oxygen plane towards a lithium vacancy. The geometry of the most stable configuration is shown in Figs. 1 and 4.

These results agree with those of a previous theoretical study [5] and those of IR polarization experiments [14].

However, they do not corroborate the result deduced from NMR measurements [9, 10, 11] on the most stable location of protons. This might be explained by noting that we have employed the structural data of undoped stoichiometric LiNbO_3 , whereas the NMR measurements of Refs. [9, 10, 11] were carried out on congruent and doped crystals.

Nevertheless, the theoretical calculations suggest that models with protons located on or nearby an O–O line are not suitable to describing the most stable OH^- defect configuration in nearly stoichiometric, hydrogen-contaminated LiNbO_3 , and they should be abandoned.

3. Summary

The geometry of OH^- defects in nearly stoichiometric, hydrogen-contaminated, LiNbO_3 has been determined from first principles theoretical calculations. In the most stable configuration the proton is located near a bisector of an oxygen triangle and is tilted by 4.3 degrees out of the oxygen plane towards a lithium vacancy (see Figs. 1 and 4). The OH^- equilibrium bond length has been found to be 0.988 Å.

Acknowledgments

The work described received support from the Hungarian Scientific Research Fund, OTKA, through the grant K60086. One of the authors, VS is indebted to Véda Vadász for encouragement and motivating discussions.

Appendix

The electronic structure calculations have been carried out using of Density Functional Theory along with the supercell method implemented in the SIESTA computational code [15]. Use has been made of norm-conserving Troullier-Martins pseudopotentials [16] and a localized basis set composed of numerical atomic orbitals of finite range. The generalized gradient approximation was employed for the exchange correlation potential. As convergence criteria of self-consistency the largest difference between the output and the input of each element of the density matrix is required to be less than 10^{-4} .

With the sample points so calculated an analytical approximation to the PES has been constructed by employing the PES reconstruction method of Ref. [17]. Specifically, with $x_1 = x, x_2 = y,$ and $x_3 = z$ denoting the three Cartesian coordinates of the proton (see Fig. 1), the PES, $V(x_1, x_2, x_3)$, is approximated as

$$V(x_1, x_2, x_3) \approx \sum_{k=1}^P c_k \prod_{i=1}^3 e^{-\alpha_i^2 \sigma_i^2 (x_{ki} - x_i)^2} \frac{\sin(2\sqrt{M_i} \sigma_i (x_{ki} - x_i))}{\sigma_i (x_{ki} - x_i)}, \quad (\text{A.1})$$

with $M_i = 1, \alpha_i = 0$ and k numbering the sample points. The linear combination coefficients c_k and the parameters σ_i have been determined such that a so called well tempered approximation be obtained. Thus of the 2251 sample points 40 randomly selected points were employed to test the quality of approximation, and the remaining $P = 2211$ points were used in constructing the analytical approximation. The approximation is well tempered when the average of the deviations of the approximating function calculated on the 2211 grid points from the exact values is nearly equal to that calculated on the 40 grid points not employed in constructing the approximating function. With $\sigma_i = 1.7768$ a well tempered approximation with average deviations of 9.48 cm^{-1} and 9.50 cm^{-1} on the 2211 sample points and on the 40 test points, respectively, has been obtained.

References

- [1] Wöhlecke M and Kovács L 2001 *Critical Reviews in Solid State and Material Sciences* **25** 29
- [2] Cabrera J M, Olivares J, Carrascosa M, Rams J, Müller R and Diéguez E 1996 *Advances in Physics* **45** 349
- [3] Yevdokimov S V and Yatsenko A V 2003 *Crystallographic Reports* **48** 542
- [4] Kovács L, Szalay V and Capelletti R 1984 *Solid State Commun.* **52** 1029
- [5] Nahm H H and Park C H 2001 *Appl. Phys. Letters* **78** 3812
- [6] Klauer S, Wöhlecke M and Kapphan S 1992 *Phys. Rev. B* **45** 2786
- [7] Lengyel K, Kovács L, Mandula G and Rupp R 2001 *Ferroelectrics* **257** 255
- [8] Ellabban A, Mandula G, Fally M, Rupp R A and Kovács L 2001 *Appl. Phys. Letters* **78** 844
- [9] Engelsberg M, de Souza R E, Pacobahyba L H and do Nascimento G C 1995 *Appl. Phys. Letters* **67** 359
- [10] Kong Y, Xu J, Zhang W and Zhang G 1998 *Phys. Letters A* **250** 211
- [11] Kong Y, Xu J, Zhang W and Zhang G 2000 *J. Phys. Chem. of Solids* **61** 1331
- [12] Abrahams S C and Marsh P 1986 *Acta Crystallogr. B* **42** 61
- [13] Szalay V, Kovács L, Wöhlecke M and Libowitzky E 2002 *Chem. Phys. Letters* **354** 56
- [14] Harrington J R, Dischler B, Räuber A and Schneider J 1973 *Solid State Commun.* **12** 351
- [15] Artacho E, Anglada E, Dieguez O, Gale J D, Garcia A, Junquera J, Martin R M, Ordejón P, Pruneda J M, Sánchez-Portal D and Soler J M 2008 *J. Phys.: Condens. Matter* **20** 064208
- [16] Martin R M 2004 *Electronic structure, Basic Theory and Practical Methods* (Cambridge: Cambridge University Press)
- [17] Szalay V 1999 *J. Chem. Phys.* **111** 8804